



# Bioinformatics and machine learning approach identifies potential drug targets and pathways in COVID-19

Md. Rabiul Auwul, Md Rezanur Rahman, Esra Gov, Md Shahjaman and Mohammad Ali Moni

Corresponding author: Mohammad Ali Moni, WHO Collaborating Centre on eHealth, UNSW Digital Health, School of Public Health and Community Medicine, Faculty of Medicine, University of New South Wales, NSW 2052, Australia. E-mail: [m.moni@unsw.edu.au](mailto:m.moni@unsw.edu.au)

## Abstract

Current coronavirus disease-2019 (COVID-19) pandemic has caused massive loss of lives. Clinical trials of vaccines and drugs are currently being conducted around the world; however, till now no effective drug is available for COVID-19. Identification of key genes and perturbed pathways in COVID-19 may uncover potential drug targets and biomarkers. We aimed to identify key gene modules and hub targets involved in COVID-19. We have analyzed SARS-CoV-2 infected peripheral blood mononuclear cell (PBMC) transcriptomic data through gene coexpression analysis. We identified 1520 and 1733 differentially expressed genes (DEGs) from the GSE152418 and CRA002390 PBMC datasets, respectively (FDR < 0.05). We found four key gene modules and hub gene signature based on module membership (MMhub) statistics and protein–protein interaction (PPI) networks (PPIhub). Functional annotation by enrichment analysis of the genes of these modules demonstrated immune and inflammatory response biological processes enriched by the DEGs. The pathway analysis revealed the hub genes were enriched with the IL-17 signaling pathway, cytokine–cytokine receptor interaction pathways. Then, we demonstrated the classification performance of hub genes (PLK1, AURKB, AURKA, CDK1, CDC20, KIF11, CCNB1, KIF2C, DTL and CDC6) with accuracy >0.90 suggesting the biomarker potential of the hub genes. The regulatory network

**Md. Rabiul Auwul** received his MSc in 2015 and BSc (honors) in 2014 in Statistics from Begum Rokeya University, Rangpur, Bangladesh. He is currently studying toward a PhD degree in Statistics at Guangzhou University, China. His research interests include data mining, robust statistics, supervised and unsupervised machine learning, system biology, transcriptomics study and bioinformatics.

**Md Rezanur Rahman** is a lecturer (on study leave) at Khwaja Yunus Ali University, Bangladesh. He is a Biotechnologist and Bioinformatician by training. He received MSc and a BSc in Biotechnology and Genetic Engineering with outstanding academic results holding the First Position in the Faculty in both degrees from Islamic University, Bangladesh. For the highest CGPA in the Faculty, he received the most prestigious award ‘Prime Minister Gold Medal 2017’ from Prime Minister of Bangladesh. He has published many research articles in internationally reputed journals. His research focuses on understanding the molecular mechanism of complex diseases utilizing systems biology and bioinformatics.

**Dr Esra Gov** received her Bachelor’s degree in Bioengineering from Ege University. Dr Gov received a PhD in Bioengineering from Marmara University, Istanbul. She is specialized in systems biology, bioinformatics and computational biology. Her interest lies in mostly biomarker identification of diseases via holistic systems medicine perspective. Dr GOV is now an assistant professor at Bioengineering Department at Adana Alparslan Turkes Science and Technology University.

**Dr Md. Shahjaman** has been working as an associate professor, Department of Statistics, Begum Rokeya University, Rangpur-5400, Bangladesh since 2010. He completed his PhD in Bioinformatics in 2018 from the University of Rajshahi, Bangladesh. He completed his BSc (honors) and MScin Statistics from the same institution. His research interest lies in theoretical and computational statistics, robust statistics, supervised and unsupervised machine learning, statistical inference, data science and deep learning with their application to big biological datasets such as biomarker identification from transcriptomics, metabolomics, and other OMICS datasets

**Dr Mohammad Ali Moni** is a senior research fellow and conjoint lecturer at WHO Collaborating Centre on eHealth and UNSW Digital Health of the University of New South Wales, Australia. Before joining the UNSW, he was a vice-chancellor fellow of the University of Sydney, Australia. He received his PhD in clinical Bioinformatics and Machine Learning from the University of Cambridge, UK. He has published over 70 peer-reviewed top tire journal articles during the last 5 years. His research interests encompass artificial intelligence, machine learning, data science, medical imaging and clinical bioinformatics.

**Submitted:** 29 December 2020; **Received (in revised form):** 15 February 2021

analysis showed transcription factors and microRNAs that target these hub genes. Finally, drug–gene interactions analysis suggests amsacrine, BRD-K68548958, naproxol, palbociclib and teniposide as the top-scored repurposed drugs. The identified biomarkers and pathways might be therapeutic targets to the COVID-19.

**Key words:** COVID-19; differentially expressed genes; gene coexpression network; systems biology; protein–protein interaction; machine learning

## Introduction

The severe acute respiratory syndrome coronavirus 2 (SARS-CoV-2) is a newly evolved virus, first identified in Wuhan, China in December 2019. Pneumonia caused by the SARS-CoV-2 was referred to as coronavirus disease (COVID-19), which was declared as the COVID-19 as a pandemic by the World Health Organization (WHO) [1]. The main symptoms of COVID-19 are fever, cough, pneumonia and shortness of breath [2]. The SARS-CoV-2 has infected almost 65 943 003 peoples with more than 1 519 137 deaths globally (as of 5 December 2020) [3].

The spread of the virus infection may be controlled through early detection of COVID-19 patients. However, the currently used methods including real-time polymerase chain reaction (RT-PCR) are subject to limited sensitivity and specificity as well as time-consuming. Moreover, careful sample collections and preparations, and skilled manpower are required, which are a tremendous drawback for developing countries. Thus, transcriptomic analysis of SARS-CoV-2 PBMC may provide candidate biomarkers. Past studies have conducted a transcriptomic analysis of various organs including lung epithelial cell [4–6], PBMC [7, 8]. Most of the previous reports detected the hub genes in COVID-19 from each module either via the PPI network or module membership criterion [5, 9–13]. Extensive gene expression analysis to identify differentially expressed genes (DEGs) and associated gene ontologies have been proposed by previous reports [5, 9–13]. Detection of specific gene modules has not been performed in COVID-19, and identification of key gene module hubs and targeting those critical genes for drugs repurposing is crucial to combat COVID-19. However, despite important findings from those studies, integrative analysis is needed to detect novel dysregulated genes and pathways for the pathogenesis of COVID-19.

The weighted gene coexpression network analysis (WGCNA) identifies significant modules (clusters) of highly correlated genes [14]. It explains the correlation patterns within genes and samples and biologically interprets the function of gene modules. The hub genes of differentially coexpressed modules provide more significance than the usual hub DEGs. WGCNA is widely used for biomarkers identification in various diseases [15–17], it has a great prospect in COVID-19. Identification of repurposable drug candidates for COVID-19 may reverse the DEGs of COVID-19, we have decided to utilize the anti-signature approach [5]. Identification of this *in silico* based approach offer opportunities to identify potential candidate drugs that might be considered for drug repositioning for COVID-19 treatment.

In this study, we implemented a system biology approach to key gene modules (identified via WGCNA) that were DEGs in COVID-19 PBMC. The hub genes were then identified from the key gene modules based on gene module membership (MMhub) and protein–protein interaction network (PPIhub), respectively. Then, we employed machine learning methods to determine the validity of these hub genes. Finally, we identified several candidate drugs considering these hub genes as therapeutic targets.

Our results may provide novel insights into the pathogenesis of COVID-19 and the potential molecular targets.

## Materials and methods

### RNA-sequencing datasets

In this study, we used two RNA-Sequencing PBMC datasets of SARS-CoV-2 (COVID-19). One of the COVID-19 gene expression raw counts dataset was obtained with the accession number GSE152418 under the platform GPL24676 from the NCBI Gene Expression Omnibus (GEO) [18]. Recently this dataset was deposited by Arunachalam et al. [7] that contained 34 samples (17 COVID-19 samples and 17 healthy control samples). The other dataset was obtained from the Chinese Academy of Science with the accession number CRA002390 that contained PBMC samples from three COVID-19 infected patients and three healthy donors [6]. In this study, the GSE152418 discovery dataset was used to analyze WGCNA, and the CRA002390 dataset was used for independent validation.

### Data preprocessing and differential gene expression analysis

The transcriptomics dataset, GSE152418, of COVID-19 contained a large number of genes (60 683 genes). For data preprocessing, the low expressed genes (sum of the gene counts for all samples <100) were excluded from this dataset. Then the differential gene expression analysis of the dataset was carried out through the DESeq2 package in the R language [19]. For the CRA002390 normalized count dataset, we used the limma package in R [20] to identify the DEGs. We considered adjusted P-value with Benjamini-Hochberg FDR correction techniques ( $FDR < 0.05$ ) and  $|\log_2(FC)| \geq 1$  statistical threshold parameters for DEGs identification.

### Weighted gene coexpression networks construction

The gene coexpression network construction was executed after removing the outlier samples (if there exist). The cluster dendrogram of the samples was constructed to check the outliers through the hclust function in R. We used the WGCNA package in R [25] to construct the weighted gene coexpression network. For finding numerous soft-thresholding powers  $\beta$  over  $R^2$ , we used the pickSoftThreshold function. Then we picked the value of  $\beta$  for which the value of  $R^2$  maximum. The adjacency matrix and Topological Overlap Matrix (TOM) were then constructed using this soft threshold power with the transformed gene expression matrix. Then the dissimilarity of TOM (dissTOM) was computed to construct a network heatmap plot and for further analyses.

For the detection of the module, the dendrogram of genes was constructed with a dissTOM matrix using hclust function with different colors. The Automerged technique was used to

get modules using the parameters:  $\text{deepSplit}=2$  and  $\text{minClusterSize}=30$  for avoiding the generation of small or large modules. Here  $\text{MEDisThres}=0.25$  was taken for merging similar modules [15].

### Preservation analysis for the key module selection

To find the key modules, we used module preservation analysis. The `modulePreservation` function [21] was used to evaluate each of the modules whether it was robust and reproducible across datasets or not. If preservation statistics  $Z$  summary  $>10$ , then the module is considered as preserved [15]. It is apparent that the module preservation and preservation statistics-median Rank are negatively correlated and there is present a positive correlation between  $Z$  summary statistic and module preservation.

### Gene ontology and pathway enrichment analysis

The high connectivity of genes inside the coexpression modules may represent crucial information about the similar biological roles within the same module. The functional enrichment analysis of the genes was studied in each selected key modules via Gene Ontology (GO) and pathway analysis [22, 23]. The GO and KEGG (Kyoto Encyclopedia of Genes and Genomes) pathway enrichment analysis was executed via the Database for Annotation, Visualization, and Integrated Discovery and visualized (DAVID) tools [24] and the result was visualized through clusterProfiler package in R [25]. A statistical threshold criterion with an adjusted  $P$ -value  $<0.05$  was used to select significant GO terms and KEGG pathways.

### Identification and validation of hub genes

In a gene module, a series of genes with the greatest degree of connectivity was detected as hub genes that investigate the characteristics of a module. Also, a module's connectivity defining the hub genes was calculated using the absolute value of the Pearson's correlation ( $|\text{cor.geneModuleMembership}| > 0.8$ ) [15]. Furthermore, we uploaded all genes of the key modules into the STRING database, choosing confidence score cutoff  $>900$  to construct protein-protein interaction (PPI). In the PPI network, genes with a connectivity degree of  $\geq 8$  were also defined as hub genes [26]. The present study further analyzed the CRA002390 validation dataset to confirm the role of these hub genes as molecular signature genes for COVID-19. The common genes among the MMhub, PPIhub and the DEGs of CRA002390 will be considered for further network analyses.

### Performance evaluation of the hub genes with classification algorithms

To check the validity of the identified common hub genes in two different analyses results (MMhub and PPIhub), the five popular classification algorithms, support vector machine (SVM) [27] radial basis kernel function, random forest (RF) [28], Poisson linear discriminant analysis (PLDA) [29], negative binomial linear discriminant analysis (NBLDA) [30] and voom-based diagonal linear discriminant analysis (voomDLDA) [31] were conducted through MLSeq package in R [32]. For the SVM and RF classifiers, we used DESeq normalization and VST transformation on the count dataset. Here, we considered the COVID-19 GSE152418 transcriptomic dataset for the classification analysis separately with MMhub genes and PPIhub genes, respectively. We computed four performance measures namely, accuracy, area under

the ROC curve (AUC), sensitivity and specificity based on the data with MMhub and PPIhub genes, respectively.

### PPI network analysis

The common genes among MMhub, PPIhub and DEGs of CRA002390 were considered for further network analysis. The PPI network for these genes was constructed via the STRING web tools [33]. STRING provides the PPI network that shows how the identified hub genes (proteins) interrelate functionally and physically with each other through encoding the gene list as input. Through the STRING information, the PPI network was constructed via Cytoscape [34] which is an open-source platform. The hub genes from this network were chosen based on degree connectivity via Cytohubba in Cytoscape. These hub genes were considered for final biomarkers of COVID-19.

### Transcription factor and miRNAs identification

The significant transcription factors (TFs) were identified through a freely accessible database of TFs repository-JASPAR [35] by executing the interaction of the TFs-target genes via NetworkAnalyst [36]. The significant miRNAs were identified from miRNAs-target gene interaction analysis through the Tarbase [37] and mirTarbase [38] database via NetworkAnalyst [36]. These networks were visualized with Cytoscape and the significant hub TFs and miRNAs were selected via the CytoHubba plugin in Cytoscape based on the degree connectivity.

### Drug-gene interaction analysis

To predict potential drugs for the treatment of COVID-19, we performed a transcriptomic anti-signature approach [5, 39] using the L1000FWD web-based tool [40], which measures the similarity score between input DEGs and expression signature and LINCS-L1000 data to detect drugs that may reverse the input gene signature. LINCS-L1000 contained drugs induced gene signature of about 50 human cell lines in response to 20 000 compounds. The significant drugs were chosen based on the criterion,  $q$ -value  $< 0.05$ .

### Proposed bioinformatics pipeline

The workflow of the proposed bioinformatics methods to identify significant pathway and drug targets were illustrated in Figure 1 with followings:

1. RNA-sequencing datasets: Differential gene expression analysis was achieved using RNA-seq data. One dataset was used to analyze the weighted gene coexpression network and the other independent dataset was used for validation.
2. Coexpression network reconstruction: The weighted gene coexpression network was constructed through the WGCNA package in R.
3. Key module selection: The Module Preservation function was used to identify robust and reproducible modules.
4. Enrichment analysis: Biological insights of key module genes were determined via the DAVID tools.
5. Hub genes identification: Hub gene signature was identified based on module membership (MMhub) statistics which calculated using the absolute value of the Pearson's correlation and PPI networks (PPIhub) by using degree metrics. The common genes as hub signature were selected among the MMhub, PPIhub and the DEGs of CRA002390..

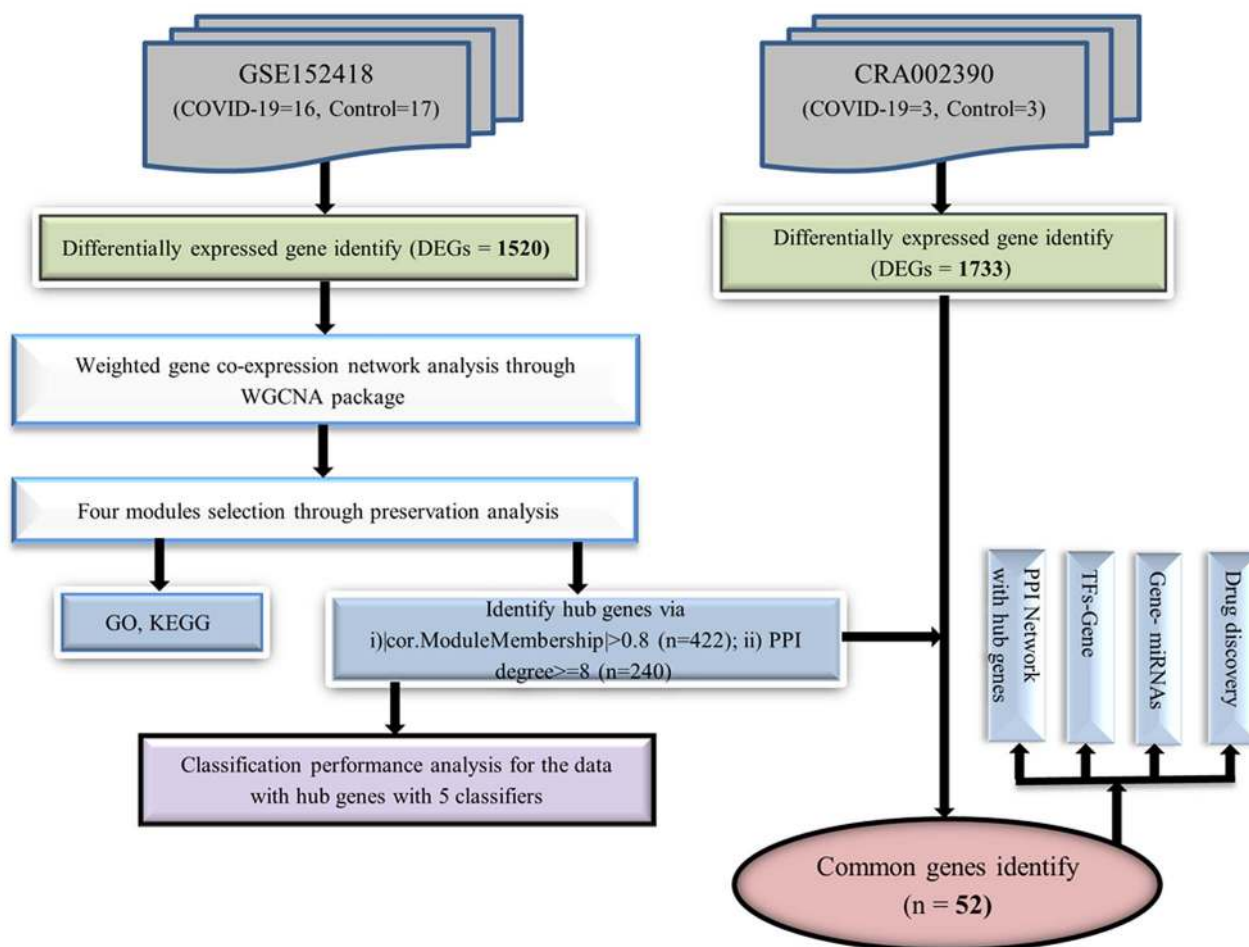


Figure 1. Flowchart of this study.

6. Validation analysis with machine learning methods: For validation of hub signatures, the five popular classification algorithms, SVM-radial basis kernel function, RF, PLDA, NBLDA and voomDLDA were conducted through MLSeq package in R.
7. Performance evaluation of hub genes: The performance measures including accuracy, AUC, sensitivity and specificity of MMhub and PPIhub genes were calculated by using an independent dataset.
8. Transcriptional regulator identification: Potential regulators (i.e.: TF and miRNA) of hub gene signature were determined using JASPAR, Tarbase and mirTarbase databases via NetworkAnalyst.
9. Candidate drug identification: LINCS-L1000 data were used to detect significant putative drugs that may reverse the input hub gene signature.

## Results

### DEGs identification

The discovery dataset (GSE152418) contained 60 683 genes with 17 COVID-19 and 17 health control samples. After excluding the lowly expressed genes, we selected 20 251 genes for DEGs

identification. We identified a total of 1520 DEGs (1299 upregulated and 221 downregulated) from this dataset (FDR < 0.05) that were considered for further weighted gene coexpression network analysis. We identified 1733 DEGs (1139 upregulated and 594 downregulated) from the validation dataset (CRA002390) in the COVID-19 samples. Table 1 presented the information regarding the datasets used in this study.

### Weighted gene coexpression networks and module preservation analysis

The gene coexpression network analyses were performed with identified 1520 DEGs of 16 COVID-19 samples in the GSE152418 dataset. The cluster dendrogram of these samples was visualized in Figure 2A that revealed, no outlying samples presented in this dataset. We selected the optimized soft-thresholding power,  $\beta = 6$  with  $R^2 = 0.90$  as the scale-free topology criteria (Figure 2B). The coexpression networks were then constructed with this soft threshold power  $\beta = 6$  and obtained 10 coexpressed modules namely, black, blue, brown, green, gray, magenta, pink, red, turquoise and yellow. The cluster dendrogram of these 10 modules presented in Figure 2D. We observed 63, 273, 259, 95, 46, 58, 77, 426 and 198 genes for black, blue, brown, green, magenta, pink, red, turquoise and yellow modules, respectively. The gray module contained 25 genes that were tied up as noncoexpressed.

**Table 1.** Overview of the COVID-19 datasets used in this study

Data accession No.	Tissue sources	# of identified DEGs	# of Samples	# of Control	# of Case
GSE152418	PBMC	1520	34	17	17 (one outlier sample)
CRA002390	PBMC	1733	6	3	3

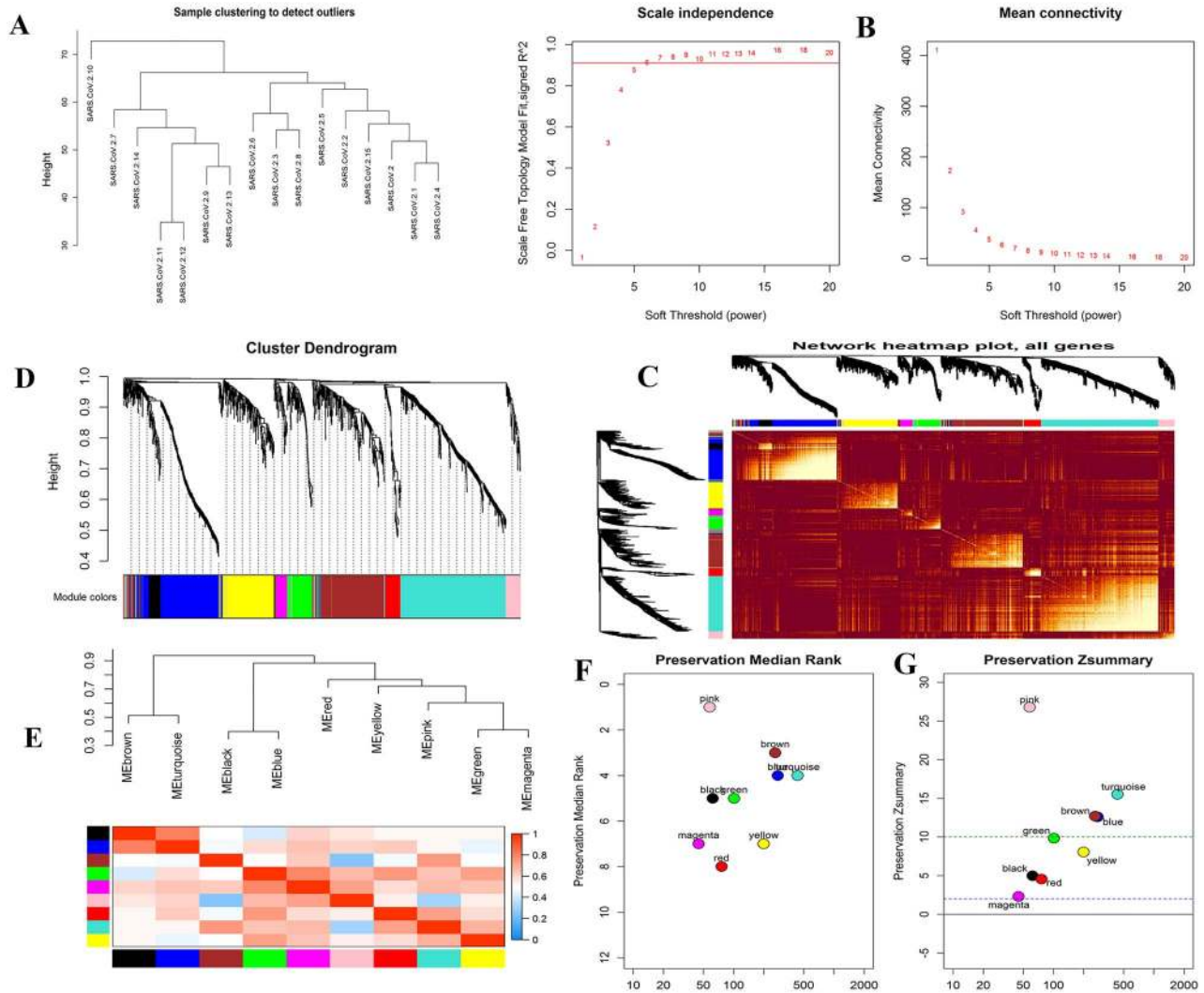


**Figure 2.** Construction of WGCNA coexpression modules and hub modules selection. (A) The cluster dendrogram of COVID-19 infected samples. (B) Analysis of the scale-free fit index (left) and the mean connectivity (right) for various soft-thresholding powers. (C) Heatmap plot of all genes. (D) Dendrogram of all differentially expressed genes clustered based on a dissimilarity measure (1-TOM). (E) Module eigengene dendrogram and eigengene network heatmap summarize the modules yielded in the clustering analysis. (F) The median rank of the modules; the rank value close to zero indicates a high degree of module preservation. (G) The Z summary statistics plot over each module; the blue and green dashed lines indicate the thresholds  $Z=2$  and  $Z=10$ , indicate moderate and strong preservation thresholds, respectively.

Figure 2C showed the network heatmap of all genes with these nine modules. The interactions among these coexpressed modules were presented with the module eigengene dendrogram and eigengene network heatmap (Figure 2E).

In the module preservation analysis, we used the GSE152418 dataset with 17 health control samples as the test dataset. We identified turquoise, blue, brown and pink modules as the most stable through preservation analysis. The remaining modules were considered nonstable since their Z summary statistic  $<10$  (Figure 2G). Figure 2F presented that the turquoise, blue, brown

and pink modules were the best-preserved among all modules since their medianRank statistic were minimum than other modules.

### Biological insights of the four-module genes

To obtain further biological insight into the genes of the selected four modules, the GO and KEGG pathway analysis was conducted in this study. The significant biological process (BP) mainly enriched in the immune response, division and fission

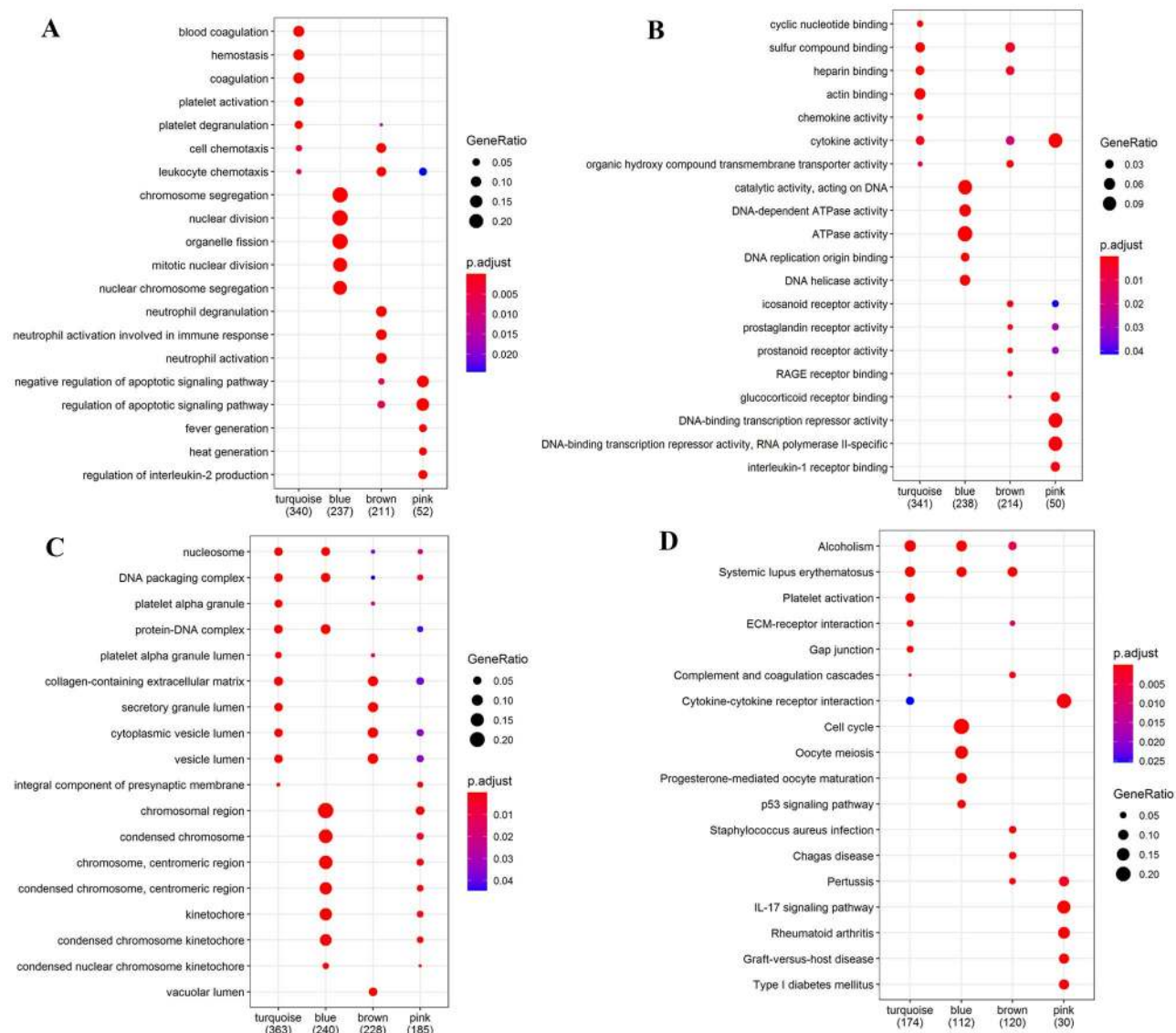


**Figure 3.** GO and KEGG enrichment analysis for four key modules. (A) biological process, (B) molecular function, (C) cellular components and (D) KEGG enrichment analysis.

related BP (Figure 3A). The significant molecular function (MF) mainly enriched in the binding related functions (Figure 3B). The most significant cellular components (CC) for the four modules are enriched in several cell compartments (Figure 3C).

The KEGG pathways for the genes of four modules significantly enriched in several pathways such as infection-related pathways (i.e: herpes simplex virus 1 infection, human papillomavirus infection), autoimmune diseases related pathways (i.e.: systemic lupus erythematosus, rheumatoid arthritis, type I diabetes mellitus), ECM-receptor interaction, IL-17 signaling pathway and p53 signaling pathway (Figure 3D and Table 2). Interestingly, alcoholism and systemic lupus erythematosus were significantly enriched for the genes of these four modules.

### Identification and validation of hub genes

We identified 422 hub genes (MMhub) in turquoise, blue, brown and pink modules with high connectivity using the module connectivity threshold criterion  $|\text{cor.geneModuleMembership}$

$> 0.8$ . Additionally, we identified 240 hub genes (PPIhub) for the four modules from the PPI through the STRING database with a connectivity degree  $\geq 8$ . The present study further analyzed the CRA002390 validation set to confirm the role of these hub genes as candidate biomarker genes for COVID-19. We identified 52 common genes among MMhub, PPIhub and the DEGs of CRA002390 (Figure 5A). The summary of these 52 genes was described in Table 4. The expression values of these common genes over the COVID-19 and health control samples were presented in Figure 5C. The heatmap showed the two main clusters of these 52 hub genes in Figure 5B in terms of COVID-19 infected samples and control samples.

### Performance evaluation of the hub genes with a classification algorithm

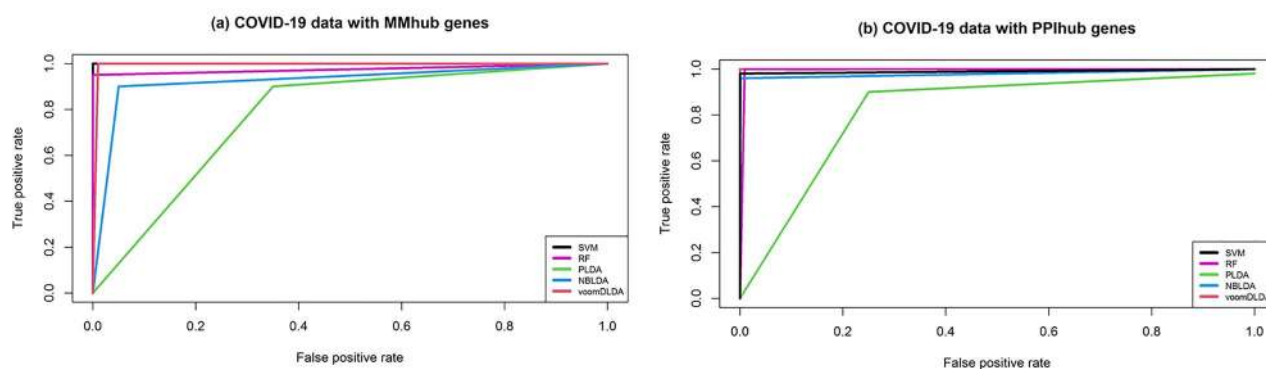
To investigate the validity of the identified hub DEGs in two different analyses (i.e.: MMhub and PPIhub), the five popular classification algorithms were executed in this study. The

Table 2. KEGG pathway enrichment results of four modules (top ten)

Modules	ID	Description	Adjusted P-value	Related genes	Count
Turquoise	hsa05034	Alcoholism	4.28E-10	HIST1H2AE,HIST1H3H,HIST1H4I;GNG11;HIST1H2AG;HIST1H2AI;HIST2H2BE HIST1H2BD;HIST1H4K;HIST1H2BJ;SLC18A2;HIST1H4H;HIST1H2AC;HIST2H4A; HIST1H2BG;HIST1H2BL;HIST1H2BK;HIST1H2BH;HIST1H2BC;HIST1H2BO; MAOB	21
	hsa05322	Systemic lupus erythematosus	5.59E-10	MYLK;GP9;GUCY1B1;ITGA2;COL1A2;PTGS1;ARHGEF12;PRKG1;VWF;GP1BA; ITGA2B;ITGB3;PLCB4;F2RL3;GP6	18
	hsa04611	Platelet activation	5.66E-08	MYLK;GP9;GUCY1B1;ITGA2;COL1A2;PTGS1;ARHGEF12;PRKG1;VWF;GP1BA; ITGA2B;ITGB3;PLCB4;F2RL3;GP6	15
	hsa04512	ECM-receptor interaction	0.000108	ITGB5;GP9;ITGA2;COL1A2;VWF;GP1BA;ITGA2B;ITGB3;GP6	9
	hsa04540	Gap junction	0.000108	EGF;GUCY1B1;PDGFA;LPAR1;PRKG1;TJP1;PLCB4;TUBB1;TUBA8	9
	hsa05203	Viral carcinogenesis	0.000123	H4C14;H2BC21;H2BC4;H2BC5;H2BC8;H2BC9;H4C8;H2BC11;H4C9;H2BC12; H2BC13;H4C12;H2BC17;CDKN2A	14
	hsa04022	cGMP-PKG signaling pathway	0.000247	OPRD1;MYLK;PDE5A;GUCY1B1;PDE2A;TRPC6;PRKG1;ADRA2A;PDE3A; SLC8A3;PLCB4;MYL9	12
	hsa04510	Focal adhesion	0.000385	MYLK;ITGB5;EGF;VEGFC;ITGA2;PDGFA;COL1A2;CAV2;VWF;BCAR1; ITGA2B;ITGB3;MYL9	13
	hsa04270	Vascular smooth muscle contraction	0.002487	PLA2G2C;MYLK;GUCY1B1;CALD1;ARHGEF12;PRKG1;PLCB4;MYL9;PPP1R14A	9
	hsa04810	Regulation of actin cytoskeleton	0.002582	IQGAP3;MYLK;ITGB5;EGF;ITGA2;PDGFA;LPAR1;ARHGEF12;BCAR1;ITGA2B; ITGB3;MYL9	12
Blue	hsa04110	Cell cycle	3.14E-24	CDC20;CDKN2C;ORC1;BUB1;MCM6;CDC25A;MCM2;MAD2L1;CCNA2;CCNB1; CDC25C;PTTG1;TTK;MCM4;CCNE2;CHEK1;CDK1;ESPL1;BUB1B;CCNB2;PKMYT1; PLK1;ORC6;CDC6;CCNE1;CDC45	26
	hsa04114	Oocyte meiosis	1.11E-13	CDC20;SPDYA;BUB1;SGO1;MAD2L1;CCNB1;CDC25C;PTTG1;FBXO5;CCNE2; FBXO43;CDK1;ESPL1;CCNB2;PKMYT1;PLK1;AURKA;CCNE1	18
	hsa04914	Progesterone-mediated oocyte maturation	1.05E-08	SPDYA;BUB1;CDC25A;MAD2L1;CCNA2;CCNB1;CDC25C;CDK1;CCNB2; PKMYT1;PLK1;AURKA	12
	hsa05322	Systemic lupus erythematosus	2.54E-06	H3C2;H2AC4;H3C3;H4C4;H4C6;H3C7;H3C8;H2AC12;H2AC14;H4C11;H3C11	11
	hsa04115	p53 signaling pathway	6.76E-06	RRM2;CCNB1;CCNE2;CHEK1;CDK1;CCNB2;CCNE1;GTSE1	8
	hsa05034	Alcoholism	9.77E-06	GNG4;H3C2;H2AC4;H3C3;H4C4;H4C6;H3C7;H3C8;H2AC12;H2AC14; H4C11;H3C11	12
	hsa05166	Human T-cell leukemia virus 1 infection	4.74E-05	CDC20;CDKN2C;MAD2L1;CCNA2;TERT;PTTG1;CCNE2;CHEK1;ESPL1; BUB1B;CCNB2;CCNE1	12
	hsa04218	Cellular senescence	5.66E-05	CDC25A;CCNA2;CCNB1;CCNE2;CHEK1;CDK1;FOXM1;CCNB2;MYBL2;CCNE1	10
	hsa03460	Fanconi anemia pathway	9.35E-05	UBE2T;RAD51;FANCI;RMI2;BRCA1;EME1	6
	hsa05203	Viral carcinogenesis	0.000115	CDC20;CCR3;CCNA2;H4C4;H4C6;H4C11;SCIN;CCNE2;CHEK1;CDK1;CCNE1	11
Brown	hsa05322	Systemic lupus erythematosus	5.01E-06	C1QA;C1QC;C1QB;FCGR1A;IL10;H2BC7;H2AC16;H3C12;H2AJ;ELANE;C3	11
	hsa05150	Staphylococcus aureus infection	0.000536	C1QA;C1QC;C1QB;FCGR1A;IL10;CAMP;C3	7
	hsa05142	Chagas disease	0.000772	C1QA;C1QC;C1QB;FASLG;IL10;TGFBR1;C3	7
	hsa05133	Pertussis	0.000889	C1QA;C1QC;C1QB;IL10;IL23A;C3	6
	hsa04610	Complement and coagulation cascades	0.001597	C1QA;C1QC;C1QB;VSIG4;CLU;C3	6
	hsa05168	Herpes simplex virus 1 infection	0.002736	FASLG;PILRB;ZNF10;ZNF597;C3;ZNF563;ZNF540;ZNF571;ZNF607;ZNF284; ZNF600;ZNF543;ZNF304;ZNF547;ZNF419;ZNF132	16
	hsa05165	Human papillomavirus infection	0.003638	FZD5;FN1;WNT7A;SPP1;ITGA1;CREB3L1;WNT11;ITGA7;CCNA1; THBS1;NOTCH3	12
	hsa05030	Cocaine addiction	0.005867	MAOA;SLC18A1;CREB3L1;GRIN3B;	4
	hsa05034	Alcoholism	0.006577	H2BC7;H2AC16;H3C12;MAOA;SLC18A1;CREB3L1;H2AJ;GRIN3B	8
	hsa04512	ECM-receptor interaction	0.009794	FN1;SPP1;ITGA1;ITGA7;THBS1	5
Pink	hsa04657	IL-17 signaling pathway	2.17E-05	IL1B;CCL20;TNF;TNFAIP3;FOSB	5
	hsa05323	Rheumatoid arthritis	0.000359	IL1A;IL1B;CCL20;TNF	4
	hsa05332	Graft-versus-host disease	0.000482	IL1A;IL1B;TNF	3
	hsa04940	Type I diabetes mellitus	0.000516	IL1A;IL1B;TNF	3
	hsa04060	Cytokine-cytokine receptor interaction	0.000639	IL1A;IL1B;CXCR4;CCL20;TNF;OSM	6
	hsa04668	TNF signaling pathway	0.000727	IL1B;CCL20;TNF;TNFAIP3	4
	hsa04380	Osteoclast differentiation	0.001199	IL1A;IL1B;TNF;FOSB	4
	hsa05162	Measles	0.001627	IL1A;IL1B;TNFAIP3;CD209	4
	hsa05418	Fluid shear stress and atherosclerosis	0.001627	IL1A;IL1B;NFE2L2;TNF	4
	hsa05321	Inflammatory bowel disease	0.00173	IL1A;IL1B;TNF	3

**Table 3.** Classification performance for the COVID-19 data with hub genes

Classifier	Data with MMhub genes				Data with PPIhub genes			
	Accuracy	AUC	Sensitivity	Specificity	Accuracy	AUC	Sensitivity	Specificity
SVM	0.996	0.997	0.996	0.998	0.986	0.989	0.996	0.981
RF	0.955	0.959	0.923	0.994	0.981	0.983	0.973	0.992
PLDA	0.821	0.848	0.902	0.794	0.768	0.815	0.930	0.700
NBLDA	0.956	0.961	0.922	0.999	0.976	0.978	0.957	0.999
voomDLDA	0.988	0.990	0.980	0.999	0.999	0.999	0.997	0.999

**Figure 4.** Receiver operating curve (ROC) plot of the five classifier performance based on (A) accuracies, (B) AUC.

performance measures have been computed based on the datasets with MMhub and PPIhub genes, respectively. We executed these calculations 20 times using 5-fold cross-validation and the average performance measurement values were computed and summarized in Table 3. The boxplot of the five machine learning classifiers based on test accuracies and AUC were presented in Figure 4. In Table 3 and Figure 4, we observed that the SVM provides greater accuracy of 0.996 than the other four classifiers (RF 0.955, PLDA 0.821, NBLDA 0.956 and voomDLDA 0.988) for the dataset with MMhub genes. We also observed that the voomDLDA provides greater accuracy of 0.999 than the other four classifiers (SVM 0.986, RF 0.981, PLDA 0.768 and NBLDA 0.976) for the dataset with PPIhub genes.

### PPI network analysis with identified common genes

The PPI networks for the 52 common genes were constructed via the STRING in Cytoscape. Figure 6A presented the network interaction among these genes and identified 10 hub genes (PLK1, AURKB, AURKA, CDK1, CDC20, KIF11, CCNB1, KIF2C, DTL and CDC6) based on a higher degree of connectivity.

### Transcriptional regulators of identified common genes

We identified 'FOXC1', 'GATA2', 'YY1', 'E2F1', 'NFIC', 'FOXL1' and 'SRF' hub TFs from the TFs-gene interaction network (Figure 6B). The significant hub miRNAs were detected from the miRNAs-gene interaction network namely, 'mir-16-5p', 'mir-124-3p', 'mir-34a-5p', 'mir-147a', 'mir-1-3p', 'mir-129-2-3p', 'mir-107' and 'mir-195-5p' (Figure 6C).

### Drug repositioning based on drug-gene overrepresentation analysis

We have identified 50 candidate drugs by reversal gene signature-based approach with  $q$ -value < 0.05. Among them, the

top 20 drugs have been summarized in Table 5. According to our analysis, 'amsacrine', 'BRD-K68548958', 'naproxol', 'palbociclib' and 'teniposide' were the top significantly identified drugs among others. These candidate drugs or components may be used for therapeutic applications in COVID-19.

## Discussion

The COVID-19 is affecting severely millions of people and taking thousands of precious lives every day over the globe due to its pandemic behavior. Though there are several candidate drugs and vaccines that were studied and proposed to treat the disease, no solid cure is available yet. The current study employed a gene coexpression network analysis to decode the critical genes and pathways of COVID-19. We identified 1520 and 1733 DEGs for the GSE152418 and CRA002390 RNA-sequencing PBMC based datasets, respectively. The four key modules were identified in GSE152418 COVID-19 data via WGCNA and module preservation analysis. The GO and pathway enrichment analysis were conducted for these key modules. We checked the validity of these identified hub genes (MMhub and PPIhub) with machine learning classifiers. We found 52 common genes in MMhub, PPIhub and the DEGs of CRA002390. The PPI networks, transcriptional regulatory networks of the common hub genes were constructed. We found 10 hub genes from the PPI of the identified common genes, and those were considered as the final candidate molecular blood signatures of COVID-19. These findings may provide new insights into the COVID-19 pathogenesis.

Our employed approach is significantly different from previous bioinformatics reports in COVID-19 research [5, 9, 12, 13, 41, 42] which relied on the identification of genes by differential analysis. However, in order to provide systems biology insights, we have implemented methodologies particularly gene coexpression module analysis that provides key gene modules



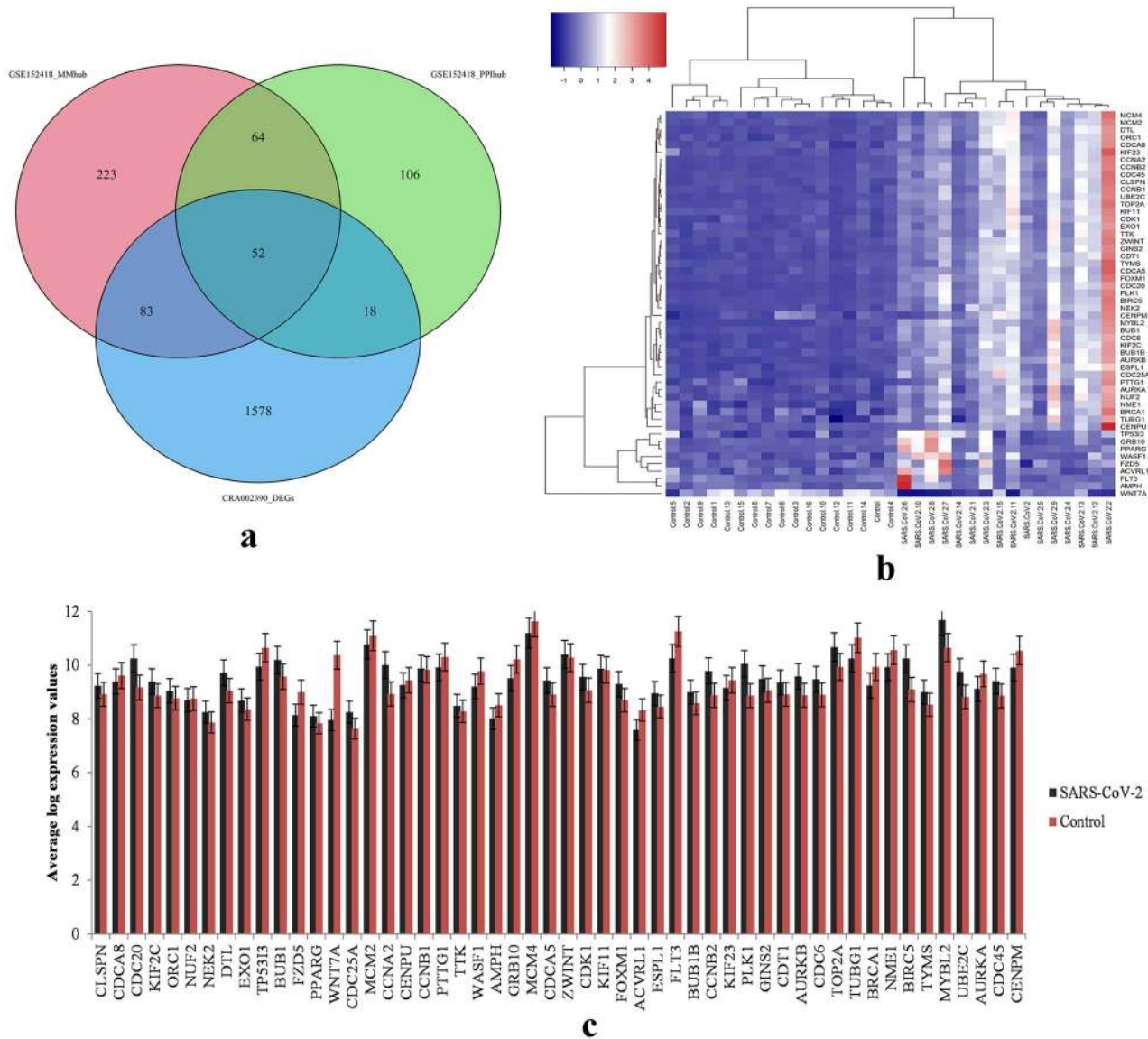


**Figure 5.** Hub gene expression profiles. (A) Venn diagram of common hub genes identified among the hub genes of GSE152418 identified via MM scores and PPI and the DEGs of CRA002390 data. (B) Heatmap of hub genes of GSE152418 dataset. (C) Bar chart of the log expression values of 52 common hub-genes in the GSE152418 dataset.

rather than finding DEGs. Firstly it clustered genes in a specific condition followed by detection of hub genes which are highly connected nodes in each module network. There is a possibility of detecting some inappropriate genes as the hub if we use only one approach. To detect the hub genes from each module more accurately, we performed joint-analysis which revealed common hub genes by module membership significance analysis and PPI analysis, which is a robust approach in selecting hub genes in COVID-19. Our analysis focused on PBMC gene expression analysis, to obtain further insights regarding the potential utilization of the identified hubs in diagnostic development for COVID-19, we decided to perform classification by widely used machine learning classifiers. The performance of state-of-the-art methods was evaluated the classification performances in which obtained a higher score in accuracy, AUC, specificity and sensitivity.

To elucidate the roles of the identified DEGs, the GO and KEGG pathway analysis were executed in this study. Among the identified GO terms, the immune response, response to cytokines, cytokine-mediated signaling and response to external stimuli play crucial roles in restricting viral infections. Among the identified pathways of four modules the cytokine-cytokine receptor interaction, the IL-17 signaling pathway was highly enriched in COVID-19. Viral infectious diseases such as herpes simplex virus 1 infection, human papillomavirus infection and viral carcinogenesis pathways were detected. Human papillomavirus infection pathways are significantly related to colorectal cancer. An autoimmune disease like rheumatoid arthritis and type 1 diabetes mellitus were also expressively enriched. These pathways show massive significance to drug repurposing chances in COVID-19.

The application of machine learning classifiers have been widely used in different bioinformatics tasks [43–45].

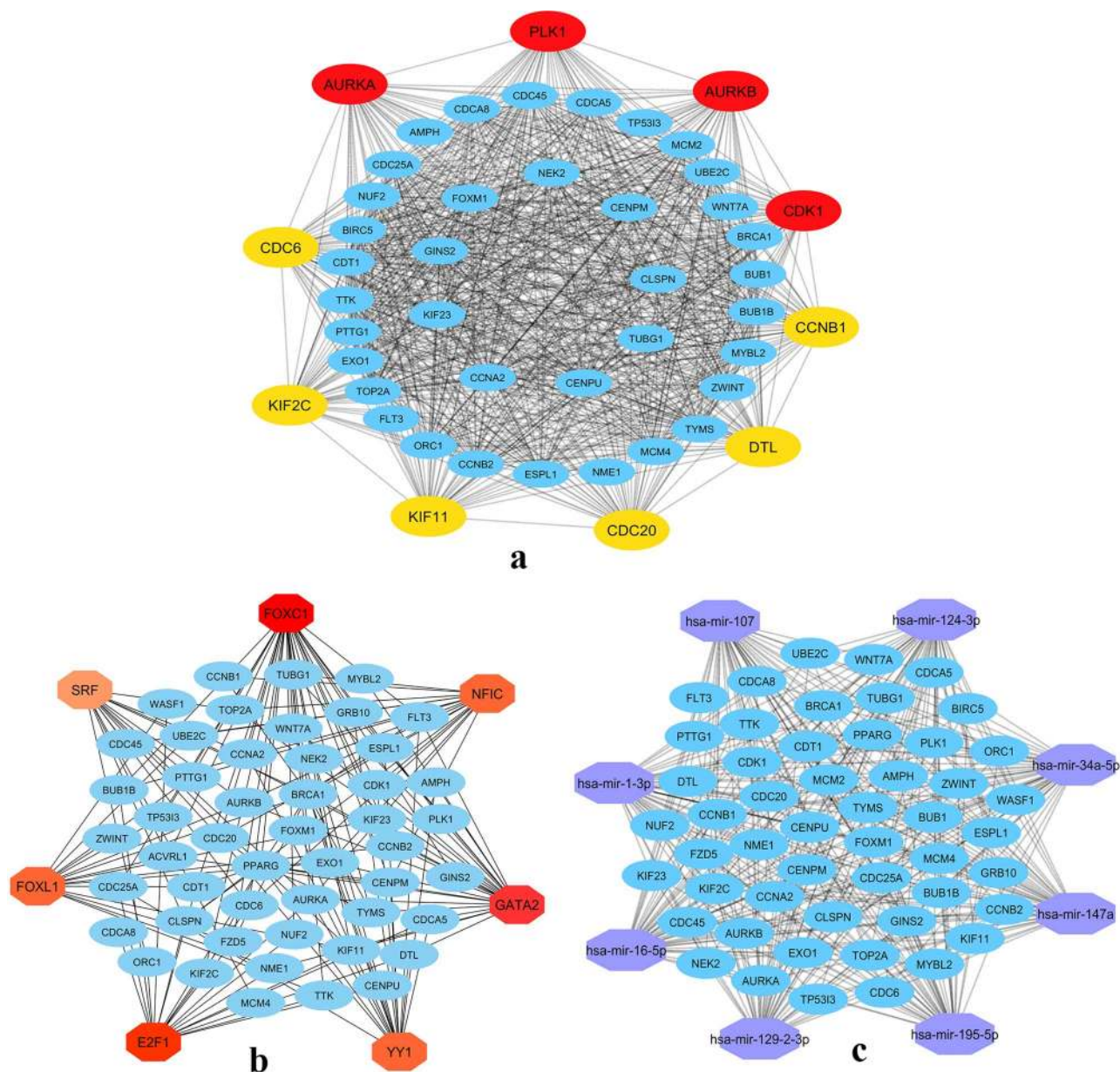


**Figure 6.** Network construction. (A) PPI network of the 52 common hub genes of COVID-19 data, (B) TFs-Gene interaction network of the 52 common hub genes, (C) gene-miRNAs interaction for the common hub genes of COVID-19.

We executed the machine learning classification algorithms based on MMhub and PPIhub genes data respectively to check their validity. We observed the satisfactory sample classification performance (accuracy >0.90; except PLDA) between COVID-19 and health control samples for both datasets (MMhub, PPIhub). The results indicate the validation of our identified hub genes through module membership and PPI networks.

We identified PLK1, AURKB, AURKA, CDK1, CDC20, KIF11, CCNB1, KIF2C, DTL and CDC6 hub genes representing that, they had a high association with clinical trait along with vital BPs and some of them were detected in COVID-19. Among them, the Polo-like kinase 1 (PLK1) gene was detected as down-regulates in Parainfluenza Virus 5 [46]. The Aurora Kinase B (AURKB) and

Aurora Kinase A (AURKA) were found SARS-CoV-2 as DEGs in Caco-2 cells [47]. The Cyclin-Dependent Kinase 1 (CDK1) genes interact with the thrombocytopenia syndrome virus which initiates the cells into the M phase [48]. The Cell Division Cycle 20 (CDC20) and CDK1 were also found as potential biomarkers for hepatocellular carcinoma [49]. The identified hub TFs and miRNAs are also significantly associated with viral infectious diseases.

Finally, we detected the candidate drugs using the reversal gene signature-based approach [5, 9]. Among them, Naproxen is a nonsteroidal anti-inflammatory drug that was studied to use for the treatment of critically COVID-19 infected patients and to limit the spread of the virus [50, 51]. The drug Teniposide was suggested to evaluate the treatment of SARS-CoV-2 infected

**Table 4.** Summary of the identified 52 genes in case of GSE152418 and CRA002390 datasets

Gene name	GSE152418		CRA002390		Gene Name	GSE152418		CRA002390	
	Log <sub>2</sub> (FC)	Adj. P-value	Log <sub>2</sub> (FC)	Adj. P-value		Log <sub>2</sub> (FC)	Adj. P-value	Log <sub>2</sub> (FC)	Adj. P-value
PLK1	3.883	7.03E-56	1.99	0.000146	KIF11	2.31	8.36E-26	2	3.24E-08
AURKB	3.22	1.57E-54	1.9	0.00184	NEK2	2.841	2.21E-25	1.61	0.000793
CCNA2	3.759	1.57E-54	1.98	7.74E-08	MCM2	1.772	4.33E-25	1.43	0.00632
UBE2C	3.571	4.50E-54	3.02	4.31E-05	CDC4A8	1.874	1.02E-23	1.48	0.00108
FOXM1	3.084	5.82E-53	1.35	0.0104	TTK	2.522	8.83E-23	2.3	9.53E-05
CDC20	3.663	3.21E-46	3.65	2.91E-12	ORC1	2.579	1.06E-21	1.23	0.00494
BIRC5	3.849	6.59E-44	3.56	2.48E-12	EXO1	2.687	1.71E-21	2.57	2.58E-07
CDT1	2.791	1.21E-42	1.7	0.0116	CDK1	2.736	6.64E-21	1.86	0.00141
DTL	3.164	8.78E-42	3.18	3.19E-05	NME1	1.207	6.67E-20	1.29	0.00863
BUB1	3.125	1.12E-38	2.96	1.97E-11	MCM4	1.638	2.22E-17	1.29	0.0173
ZWINT	2.375	3.09E-38	2.49	7.28E-05	CENPU	1.955	1.25E-15	1.57	3.28E-05
GINS2	2.812	9.82E-37	1.74	0.011	KIF23	1.797	5.57E-15	2.47	5.05E-11
CCNB2	3.433	2.69E-36	2.89	1.43E-09	AURKA	1.396	5.91E-15	2.02	2.43E-05
CLSPN	2.652	5.78E-35	1.42	0.00244	PTTG1	1.577	7.69E-14	1.04	0.0383
TYMS	2.98	4.83E-33	2.53	3.05E-05	TUBG1	1.007	2.35E-13	1.54	0.000929
MYBL2	3.442	1.22E-32	3.45	2.91E-12	PPARG	3.169	4.61E-11	5.52	3.68E-07
CDC45	3.039	2.51E-32	2.95	3.67E-06	CENPM	1.212	8.67E-11	1.67	0.0139
CDC6	2.948	2.51E-32	2.32	2.85E-06	BRCA1	1.128	1.95E-10	1.08	0.0261
TOP2A	3.174	6.24E-31	2.58	5.48E-10	WASF1	1.503	2.10E-08	2.44	0.00218
CDC45	2.869	8.03E-31	3.38	2.37E-11	TP53I3	1.175	1.19E-06	2.05	0.00108
ESPL1	2.805	1.38E-30	2.68	3.48E-07	GRB10	1.636	2.22E-06	3.82	4.48E-05
BUB1B	2.79	6.29E-30	2.45	2.34E-09	AMPH	1.853	4.06E-06	4.1	0.000303
KIF2C	2.909	8.87E-30	2.01	4.81E-05	FZD5	1.205	6.73E-05	2.57	0.000514
CCNB1	2.292	4.88E-29	2.06	3.27E-07	ACVRL1	1.38	0.00033	3.89	0.000105
CDC25A	3.101	1.13E-28	4.05	4.44E-14	WNT7A	-1.036	0.002901	-2.27	0.0445
NUF2	2.131	4.41E-26	1.55	9.15E-05	FLT3	1.33	0.003703	4.7	4.36E-05

**Table 5.** Candidate drugs (top twenty) identified from gene–drug interaction enrichment analysis

Drug	Similarity score	P-value	q-value	z-score	Combined score
Amsacrine	-0.7143	1.23E-48	1.32E-44	1.69	-80.79
BRD-K68548958	-0.7143	5.98E-50	1.28E-45	1.82	-89.76
Naproxol	-0.6939	8.02E-47	5.72E-43	1.69	-77.84
Palbociclib	-0.6939	3.47E-46	1.65E-42	1.61	-72.96
SIB-1893	-0.6939	7.00E-47	5.72E-43	1.67	-77.09
ZK-164015	-0.6939	5.46E-46	2.12E-42	1.67	-75.62
Tanespimycin	-0.6939	4.22E-46	1.81E-42	1.63	-74.15
Emodic-acid	-0.6939	9.83E-47	6.01E-43	1.7	-78
BRD-K29506255	-0.6735	4.27E-45	1.52E-41	1.78	-78.99
Teniposide	-0.6531	8.98E-43	2.13E-39	1.68	-70.64
Diphenyleneiodonium	-0.6531	3.33E-42	7.14E-39	1.64	-67.86
Homosalate	-0.6531	2.30E-42	5.19E-39	1.68	-70.07
SIB-1893	-0.6531	6.11E-43	1.54E-39	1.68	-70.75
Ingenol	-0.6327	3.52E-40	5.79E-37	1.75	-69.13
FCCP	-0.6327	5.36E-41	9.98E-38	1.83	-73.81
Tremulacin	-0.6122	3.84E-39	4.98E-36	1.74	-66.81
BRD-K30836161	-0.6122	4.89E-39	6.16E-36	1.76	-67.42
Idarubicin	-0.6122	2.67E-38	3.09E-35	1.59	-59.71
Wortmannin	-0.6122	9.75E-40	1.49E-36	1.84	-71.72
Devazepide	-0.6122	4.20E-38	4.73E-35	1.64	-61.18

patients [52]. We proposed to send these candidate drugs for biological and clinical experimentation for the possible use in COVID-19 treatment.

Our analysis focused on PBMC gene expression analysis, to obtain further insights regarding the potential utilization of the identified hubs in diagnostic development for COVID-19, we decided to perform classification by widely used machine

learning classifiers. Our analysis showed a good level of specificity in classification performances.

However, several limitations of the study should be noted as findings of this study relied on bioinformatics analysis without functional studies in wet-lab, thus caution should be taken in interpreting the results. Moreover, the transcriptomic analysis and candidate drugs were identified by reversal of PBMC

gene expression in COVID-19 but the primary affected organ by SARS-CoV-2 is lung tissues, thus further research is now proposed to explore biological insights in COVID-19.

## Conclusions

The present research aimed to identify key genes and molecular pathways altered in response to SARS-CoV-2 in blood cells compared to normal blood cells. We detected four key modules through module preservation analysis. The 52 common genes were identified from resultant 422 and 240 hub genes based on module membership statistics and PPI networks and from 1733 detected DEGs of CRA002390. The 10 hub genes (PLK1, AURKB, AURKA, CDK1, CDC20, KIF11, CCNB1, KIF2C, DTL and CDC6) were identified from the PPI networks of these 52 genes. The TFs (FOXC1, GATA2, YY1, E2F1, NFIC, FOXL1 and SRF) were also found as potential regulators of the hub genes. The naproxol, teniposide, amsacrine, BRD-K68548958, palbociclib were identified as the top-scored repurposed drugs for COVID-19 pathogenesis. The identified drugs should be judged with wet-lab experiments before clinical studies. Our results may provide novel insights into the pathogenesis of COVID-19 and the potential molecular targets for novel interventional approaches.

### Key Points

- COVID-19 pandemic has emerged as a massive threat to humankind limited by the unavailability of effective drugs.
- This study has performed a comprehensive clinical bioinformatics and systems biology analysis of all available SARS-CoV-2 infected peripheral blood mononuclear cell (PBMC) transcriptomic datasets to identify gene modules by gene coexpression analysis.
- A robust four key gene modules and hub gene signature were detected based on gene module membership statistics and protein-protein interaction networks and machine learning methods.
- Functional annotation by enrichment analysis of the genes of these modules demonstrated immune and inflammatory response biological processes enriched by the gene signature.
- Several potential candidate drugs based on the reversal of transcriptomic signature were also detected that may be effective treatment candidate for COVID-19.

## Acknowledgments

Not applicable.

## Funding

No funding received for this study.

## Data availability

All data utilized in this manuscript are available online from their respective database.

## References

1. Cucinotta D, Vanelli M. WHO declares COVID-19 a pandemic. *Acta Biomed* 2020;**90**:157–60.
2. Chen N, Zhou M, Dong X, et al. Epidemiological and clinical characteristics of 99 cases of 2019 coronavirus pneumonia in Wuhan, China: a descriptive study. *Lancet* 2020;**395**: 507–13.
3. Ahamad MM, Aktar S, Rashed-Al-Mahfuz M, et al. A machine learning model to identify early stage symptoms of SARS-Cov-2 infected patients. *Expert systems with applications* 2020;**160**:113661.
4. Blanco-Melo D, Nilsson-Payant B, Liu W-C, et al. SARS-CoV-2 launches a unique transcriptional signature from in vitro, ex vivo, and in vivo systems. *bioRxiv* 2020 March 24, 2020. doi: [10.1101/2020.03.24.004655](https://doi.org/10.1101/2020.03.24.004655) Arxiv biorxiv;2020.03.24.004655v1, preprint: not peer reviewed.
5. Islam T, Rahman MR, Aydin B, et al. Integrative transcriptomics analysis of lung epithelial cells and identification of repurposable drug candidates for COVID-19. *Eur J Pharmacol* 2020;**887**:173594.
6. Xiong Y, Liu Y, Cao L, et al. Transcriptomic characteristics of bronchoalveolar lavage fluid and peripheral blood mononuclear cells in COVID-19 patients. *Emerg Microbes Infect* 2020;**9**:761–70.
7. Arunachalam PS, Wimmers F, Mok CKP, et al. Systems biological assessment of immunity to mild versus severe COVID-19 infection in humans. *Science (80-)* 2020;**369**:1210–20.
8. Ong EZ, Fu Y, Chan Z, et al. A dynamic immune response shapes COVID-19 progression. *Cell Host Microbe* 2020;**27**:879–882.e2.
9. Fagone P, Ciurleo R, Lombardo SD, et al. Transcriptional landscape of SARS-CoV-2 infection dismantles pathogenic pathways activated by the virus, proposes unique sex-specific differences and predicts tailored therapeutic strategies. *Autoimmun Rev* 2020;**19**:102571.
10. Dolan M, Hill D, Mukherjee G, et al. Investigation of COVID-19 comorbidities reveals genes and pathways coincident with the SARS-CoV-2 viral disease. *Sci Rep* 2020;**10**:20848.
11. Satu MS, Khan MI, Rahman MR, et al. Disease and comorbidities complexities of SARS-CoV-2 infection with common malignant diseases. *Brief Bioinform* 2021;**22**:1415–29.
12. Moni MA, Quinn JMW, Sinmaz N, et al. Gene expression profiling of SARS-CoV-2 infections reveal distinct primary lung cell and systemic immune infection responses that identify pathways relevant in COVID-19 disease. *Brief Bioinform* 2020;**22**:1324–37.
13. Nashiry A, Sarmin Sumi S, Islam S, et al. Bioinformatics and system biology approach to identify the influences of COVID-19 on cardiovascular and hypertensive comorbidities. *Brief Bioinform* 2021;**22**:1387–401.
14. Langfelder P, Horvath S. WGCNA: an R package for weighted correlation network analysis. *BMC Bioinformatics* 2008;**9**:559.
15. Jin X, Li J, Li W, et al. Weighted gene co-expression network analysis reveals specific modules and biomarkers in Parkinson's disease. *Neurosci Lett* 2020;**728**:134950.
16. Iu R, Zhang W, Liu Z, et al. Associating transcriptional modules with colon cancer survival through weighted gene co-expression network analysis. *BMC Genomics* 2017;**18**:361.
17. Feng T, Li K, Zheng P, et al. Weighted gene coexpression network analysis identified MicroRNA coexpression modules and related pathways in type 2 diabetes mellitus. *Oxid Med Cell Longev* 2019;**2019**:1–12.

18. Barrett T, Wilhite SE, Ledoux P, et al. NCBI GEO: archive for functional genomics data sets—update. *Nucleic Acids Res* 2013;**41**:991–5.
19. Love MI, Huber W, Anders S. Moderated estimation of fold change and dispersion for RNA-seq data with DESeq2. *Geneome Biol* 2014;**15**:550.
20. Ritchie ME, Phipson B, Wu D, et al. Limma powers differential expression analyses for RNA-sequencing and microarray studies. *Nucleic Acids Res* 2015;**43**:e47.
21. Langfelder P, Luo R, Oldham MC, et al. Is my network module preserved and reproducible? *PLoS Comput Biol* 2011;**7**:e1001057 e1001057
22. Rahman MH, Rana HK, Peng S, et al. Bioinformatics and machine learning methodologies to identify the effects of central nervous system disorders on glioblastoma progression. *Brief Bioinform* 2021;bbaa365.
23. Rahman MR, Islam T, Nicoletti F, et al. Identification of common pathogenetic processes between schizophrenia and diabetes mellitus by systems biology analysis. *Genes (Basel)* 2021;**12**:237.
24. Huang d W, Sherman BT, Lempicki RA. Systematic and integrative analysis of large gene lists using DAVID bioinformatics resources. *Nat Protoc* 2009;**4**:44–57.
25. Yu G, Wang L, Han Y, et al. clusterProfiler: an R package for comparing biological themes among gene clusters. *Omi A J Integr Biol* 2012;**16**:284–7.
26. Yuan L, Chen L, Qian K, et al. Co-expression network analysis identified six hub genes in association with progression and prognosis in human clear cell renal cell carcinoma (ccRCC). *Genomics Data* 2017;**14**:132–40.
27. Boser B, Guyon I, Vapnik V. A training algorithm for optimal margin classes. *Proc. 5th Annu. Work. Comput. Learn. theory* 1992; 144–52
28. Ho TK. Random decision forests. *Proc. Int. Conf. Doc. Anal. Recognition, ICDAR* 1995; 1:278–82
29. Witten DM. Classification and clustering of sequencing data using a Poisson model. *Annals of Applied Statistics* 2011;**5**:2493–518.
30. Dong K, Zhao H, Tong T, et al. NBLDA: negative binomial linear discriminant analysis for RNA-Seq data. *BMC Bioinf* 2016;**17**:369.
31. Dudoit S, Fridlyand J, Speed TP. Comparison of discrimination methods for the classification of tumors using gene expression data. *J Am Stat Assoc* 2002;**97**:77–87.
32. Goksuluk D, Zararsiz G, Korkmaz S, et al. MLSeq: machine learning interface for RNA-sequencing data. *Comput Methods Programs Biomed* 2019;**175**:223–31.
33. Szklarczyk D, Morris JH, Cook H, et al. The STRING database in 2017: quality-controlled protein-protein association networks, made broadly accessible. *Nucleic Acids Res* 2017;**45**:D362–8.
34. Smoot ME, Ono K, Ruscheinski J, et al. Cytoscape 2.8: new features for data integration and network visualization. *Bioinformatics* 2011;**27**:431–2.
35. Khan A, Fornes O, Stigliani A, et al. JASPAR 2018: update of the open-access database of transcription factor binding profiles and its web framework. *Nucleic Acids Res* 2018;**46**:D260–6.
36. Xia J, Gill EE, Hancock REW. NetworkAnalyst for statistical, visual and network-based meta-analysis of gene expression data. *Nat Protoc* 2015;**10**:823–44.
37. Sethupathy P, Corda B, Hatzigeorgiou AG. TarBase: a comprehensive database of experimentally supported animal microRNA targets. *RNA* 2006;**12**:192–7.
38. Hsu S-D, Lin F-M, Wu W-Y, et al. miRTarBase: a database curates experimentally validated microRNA–target interactions. *Nucleic Acids Res* 2011;**39**:D163–9.
39. Rahman MR, Islam T, Gov E, et al. Identification of prognostic biomarker signatures and candidate drugs in colorectal cancer: insights from systems biology analysis. *Medicina (Kaunas)* 2019;**55**:20.
40. Wang Z, Lachmann A, Keenan AB, et al. L1000FWD: fireworks visualization of drug-induced transcriptomic signatures. *Bioinformatics* 2018;**34**:2150–2.
41. Li X, Yu J, Zhang Z, et al. Network bioinformatics analysis provides insight into drug repurposing for COVID-2019 Preprints. 2019.
42. Feng Z, Chen M, Liang T, et al. Virus-CKB: an integrated bioinformatics platform and analysis resource for COVID-19 research. *Brief Bioinform* 2020;**22**:882–95.
43. Hasan MM, Schaduangrat N, Basith S, et al. HLPpred-fuse: improved and robust prediction of hemolytic peptide and its activity by fusing multiple feature representation. *Bioinformatics* 2020;**36**:3350–6.
44. Hasan MM, Khatun MS, Kurata H. iLBE for computational identification of linear B-cell epitopes by integrating sequence and evolutionary features. *Genomics Proteomics Bioinformatics* 2020.
45. Hasan MM, Basith S, Khatun MS, et al. Meta-i6mA: an interspecies predictor for identifying DNA N6-methyladenine sites of plant genomes by exploiting informative features in an integrative machine-learning framework. *Brief Bioinform* 2020;bbaa202.
46. Sun D, Luthra P, Li Z, et al. PLK1 down-regulates parainfluenza virus 5 gene expression. *PLoS One* 2009;**5**:e1000525.
47. Bock J-O, Ortea I. Re-analysis of SARS-CoV-2-infected host cell proteomics time-course data by impact pathway analysis and network analysis: a potential link with inflammatory response. *Aging (Albany NY)* 2020;**12**:11277–86.
48. Su M, Chen Y, Qi S, et al. A mini-review on cell cycle regulation of coronavirus infection. *Front Vet Sci* 2020;**7**:943.
49. Yang W-X, Pan Y-Y, You C-G. CDK1, CCNB1, CDC20, BUB1, MAD2L1, MCM3, BUB1B, MCM2, and RFC4 may be potential therapeutic targets for hepatocellular carcinoma using integrated bioinformatic analysis. *Biomed Res Int* 2019;**2019**:16 pp.
50. Efficacy of addition of naproxen in the treatment of critically ill patients hospitalized for COVID-19 infection (ENACOVID). 2020.
51. Oany AR, Mia M, Pervin T, et al. Design of novel viral attachment inhibitors of the spike glycoprotein (S) of severe acute respiratory syndrome coronavirus-2 (SARS-CoV-2) through virtual screening and dynamics. *International journal of antimicrobial agents* 2020;**56**:106177.
52. Bharadwaj S, Azhar EI, Amjad Kamal M, et al. SARS-CoV-2 Mpro inhibitors: identification of anti-SARS-CoV-2 Mpro compounds from FDA approved drugs. *J Biomol Struct Dyn* 2020;**38**:1–16.